

## A Small Synthetic Molecule Functions as a Chloride-Bicarbonate Dual-Transporter and Induces Chloride Secretion in Cells

 Peng-Yun Liu,<sup>a</sup> Shing-To Li,<sup>a</sup> Fang-Fang Shen,<sup>a</sup> Wing-Hung Ko,<sup>b\*</sup> Xiao-Qiang Yao,<sup>b\*</sup> and Dan Yang<sup>a\*</sup>

 Received 00th January 20xx,  
Accepted 00th January 20xx

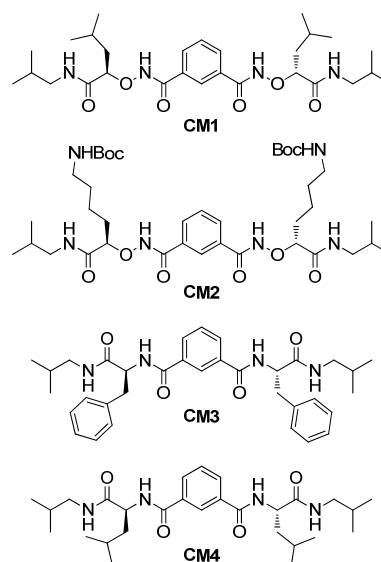
[www.rsc.org/](http://www.rsc.org/)

A C<sub>2</sub> symmetric small molecule composed of L-phenylalanine and isophthalamide was found to function as a Cl<sup>-</sup>/HCO<sub>3</sub><sup>-</sup> dual transporter and self-assemble into chloride channel. In Ussing-chamber based short-circuit current measurements, this molecule elicited chloride-dependent short-circuit current (I<sub>sc</sub>) increase in both Calu-3 cell and CFBE410- cell (with F508del mutant CFTR) monolayers.

Bicarbonate (HCO<sub>3</sub><sup>-</sup>) plays important roles in biological processes including photosynthesis, the Krebs cycle, whole-body and cellular pH regulation, and volume regulation<sup>1</sup>. In mammals, movement of bicarbonate across cell membrane is facilitated by fourteen bicarbonate transporters, including anion exchanger (AE) family, Na<sup>+</sup>/HCO<sub>3</sub><sup>-</sup> co-transport (NBC) family, and Na-driven Cl<sup>-</sup>/HCO<sub>3</sub><sup>-</sup> exchangers (NDCBE), which drive HCO<sub>3</sub><sup>-</sup> metabolism<sup>2</sup>. Dysregulation of bicarbonate transport can lead to conditions such as cystic fibrosis<sup>3</sup>, heart disease and infertility<sup>4</sup>. Previously, we discovered that small C<sub>2</sub>-symmetric molecule with an isophthalamide scaffold linking two R-(α)-aminoxy leucine units (**CM1**) was capable of self-assembling into selective Cl<sup>-</sup> channels<sup>5</sup>, and the isophthalamide scaffold linking two Boc-protected (α)-aminoxy lysine residues (**CM2**), can self-assemble into K<sup>+</sup> channels in liposomes and living cell membranes (Scheme 1)<sup>6</sup>. As α-aminoxy acids have different conformational preference from regular α-amino acids, it will be interesting to explore if the replacement of the α-aminoxy acid residues in both **CM1** and **CM2** by corresponding α-amino acid residues would affect their ion transport activities. Herein, we report small molecule **CM3**, which has an isophthalamide scaffold linking two α-phenylalanine residues, can form chloride channels and mediate chloride/bicarbonate transport in liposomes.

Compared with our previously studies, **CM3** possesses simplified synthetic route and much higher transport abilities. While most studies on Cl<sup>-</sup>/HCO<sub>3</sub><sup>-</sup> transporters have been focused on their anticancer properties<sup>7</sup>, we demonstrate here that **CM3** mediates chloride and bicarbonate transport across Calu-3 monolayers and restores dysfunctional chloride secretion across CFBE410- monolayers.

Firstly, we used the pH-sensitive fluorescent dye 8-hydroxy-1,3,6-pyrene-trisulfonate (HPTS, pyranine) to test the ion transport property of compounds **CM3** and **CM4** (an α-leucine analog of **CM3**). HPTS and NaCl encapsulated liposomes were suspended in an isotonic NaCl solution. Then a testing compound and a NaOH base pulse were added to the extravesicular solution. The resulting pH gradient caused by the base pulse drove the efflux of protons or influx of hydroxide ions and built up a transmembrane electrostatic potential. This



Scheme 1. Chemical Structures of channel forming molecules.

<sup>a</sup> Morningside Laboratory for Chemical Biology, Department of Chemistry, The University of Hong Kong, Pokfulam Road, Hong Kong, P. R. China. E mail: yangdan@hku.hk.

<sup>b</sup> School of Biomedical Sciences, The Chinese University of Hong Kong, Shatin, N.T., Hong Kong, P. R. China. E mail: whko@cuhk.edu.hk; yao2068@cuhk.edu.hk.

†Electronic Supplementary Information (ESI) available: Experimental procedures, characterization data, and NMR spectra of new compounds (PDF). See DOI: 10.1039/x0xx00000x

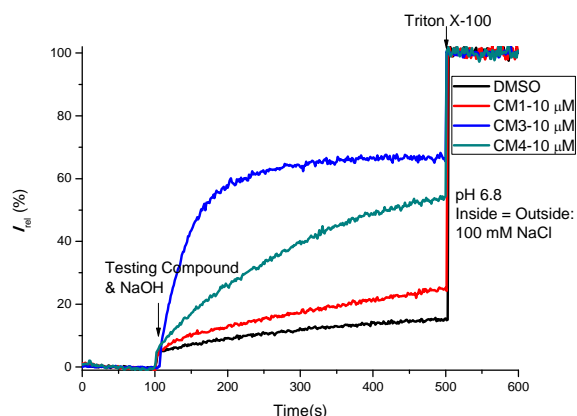


Figure 1. HPTS base pulse assay of channel forming molecules. Inside vesicles: 100 mM NaCl, 0.1 mM HPTS, 10 mM HEPES, pH 6.8. Outside vesicles: 100 mM NaCl, 10 mM HEPES, pH 6.8. At  $t = 100$  s, DMSO (20  $\mu$ L, negative control) or DMSO solution of testing compound (20  $\mu$ L, 10  $\mu$ M final concentration) was added, followed by the addition of a NaOH aqueous solution (20  $\mu$ L, 0.5 M). At  $t = 500$  s, 40  $\mu$ L of 5% Triton X-100 was added to lyse the liposomes.

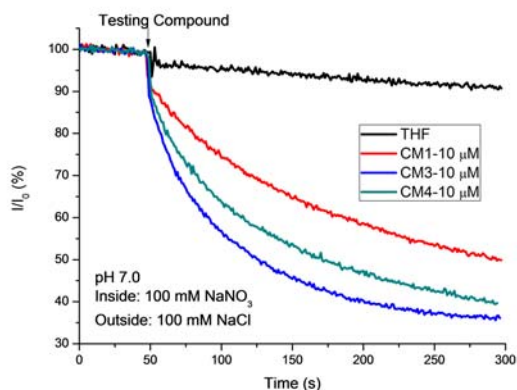


Figure 2. SPQ chloride transport assay. Inside vesicles: 200 mM NaNO<sub>3</sub>, 0.5 mM SPQ, 10 mM HEPES, pH 7.0. Outside vesicles: 200 mM NaCl, 10 mM HEPES, pH 7.0. At  $t = 50$  s, THF (20  $\mu$ L, negative control) or a THF solution of **CM1**, **CM3** or **CM4** (20  $\mu$ L, 10  $\mu$ M final concentration) was added.

electrostatic potential could be compensated, if the testing compound mediated anion efflux or cation influx and a subsequent continuous HPTS fluorescence change would be recorded. As shown in Figure 1, by replacing the  $\alpha$ -aminoxy acid residue of **CM1** to  $\alpha$ -amino acid residue, **CM4** surprisingly mediated a more efficient electrolyte exchange. Further side-chain modification from leucine to phenylalanine enable **CM3** to induce a more rapid increase in HPTS fluorescence than **CM4**.

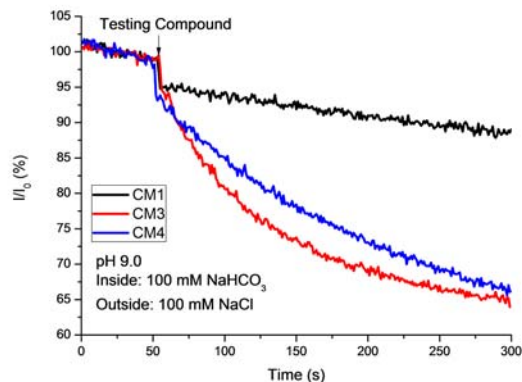


Figure 3. SPQ assay on Cl<sup>-</sup>/HCO<sub>3</sub><sup>-</sup> exchange across liposome lipid bilayers. Inside vesicles: 100 mM NaHCO<sub>3</sub>, 0.5 mM SPQ, pH 9.0; outside vesicles: 100 mM NaCl, 5 mM Tris, pH 9.0. At  $t = 50$  s, THF (20  $\mu$ L, negative control) or a THF solution of **CM1**, **CM3** or **CM4** (20  $\mu$ L, 20  $\mu$ M final concentration) was added.

To explore the ionic origin of electrolyte exchange in the HPTS assay, another HPTS assay in Na<sub>2</sub>SO<sub>4</sub> solution was carried out (Figure S1). No continuous HPTS fluorescence change was recorded, suggesting no Na<sup>+</sup> transport in this assay. We then used the halide-sensitive fluorescent indicator, 6-methoxy-*N*-(3-sulfo-propyl) quinolinium (SPQ)<sup>8</sup>, to compare the chloride transport property of **CM1**, **CM3** and **CM4** (Figure 2). NaNO<sub>3</sub> and SPQ encapsulated liposomes were suspended in an isotonic NaCl solution<sup>5a</sup>. Interestingly, **CM3** and **CM4** induced a more rapid decrease of the fluorescence of SPQ than **CM1**, indicating more efficient Cl<sup>-</sup> influx mediated by **CM3** and **CM4**.

Next, we used SPQ assay to investigate the Cl<sup>-</sup>/HCO<sub>3</sub><sup>-</sup> exchange property of **CM1**, **CM3** and **CM4**. Liposomes encapsulating NaHCO<sub>3</sub> and SPQ were suspended in an isotonic NaCl solution at pH 9.0. In contrast to **CM1**, both **CM3** and **CM4** induced a decrease in the fluorescence of SPQ, indicating Cl<sup>-</sup>/HCO<sub>3</sub><sup>-</sup> exchange mediated by **CM3** and **CM4**, but not by **CM1** (Figure 3).

Since **CM3** exhibited higher transport activity than **CM4** in both Cl<sup>-</sup> transport and Cl<sup>-</sup>/HCO<sub>3</sub><sup>-</sup> exchange in liposome assays, **CM3** was chosen for further characterization experiments. Patch-clamp study involving single-channel recording was the most critical test for ion channel formation<sup>9</sup>. The characteristic single-channel current was recorded in the presence of 10  $\mu$ M **CM3** in a bath solution of symmetric 150 mM NaCl (Figure 4) or symmetric 150 mM *N*-methylglucamine hydrochloride (NMDG-Cl; Figure S2), indicating the formation of functional chloride ion channel within the lipid bilayers of liposomes. In addition, the relative ion permeability of Cl<sup>-</sup> over Na<sup>+</sup> was determined to be  $7.4 \pm 2.1$  (Figure S3). Thus, our patch clamp results were consistent with that from SPQ fluorescence experiments, further confirming that **CM3** indeed forms chloride channel in lipid bilayer.

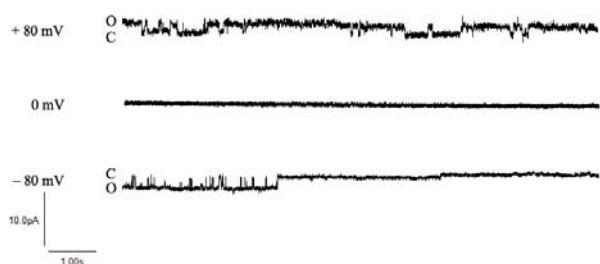


Figure 4. Typical single channel currents of self-assembled channels were recorded in the presence of **CM3** at 10  $\mu\text{M}$ , when both intra- and extravesicular solutions were symmetric 150 mM NaCl.

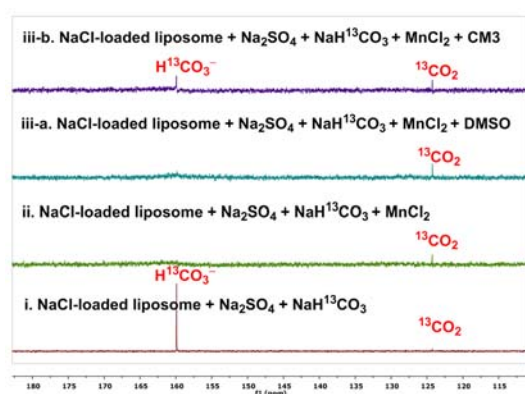


Figure 5.  $^{13}\text{C}$ -NMR spectroscopy experiments demonstrated that **CM3** facilitated bicarbonate influx into vesicles. NaCl-encapsulated liposomes were suspended in a  $\text{Na}_2\text{SO}_4$  solution. The intravesicular solution contained 450 mM NaCl and 20 mM HEPES (pH 7.3), and the extravesicular solution contained 150 mM  $\text{Na}_2\text{SO}_4$  and 20 mM HEPES (pH 7.3). (i) The  $^{13}\text{C}$ -NMR spectrum was obtained after the addition of  $\text{NaH}^{13}\text{CO}_3$  to the extravesicular solution. (ii) The  $^{13}\text{C}$ -NMR spectrum was obtained after the addition of 0.5 mM  $\text{Mn}^{2+}$  ( $1/100 = [\text{Mn}^{2+}]/[\text{H}^{13}\text{CO}_3^-]$ ). (iii-a) The  $^{13}\text{C}$ -NMR spectrum was obtained after the addition of DMSO to the solution obtained in step ii. (iii-b) The  $^{13}\text{C}$ -NMR spectrum was obtained after the addition of **CM3** to the solution obtained in step ii (**CM3** in DMSO, 1% relative to lipid, the same volume as the DMSO added in step iii-a).

The direct evidence for transmembrane  $\text{HCO}_3^-$  transport facilitated by **CM3** was obtained by the liposome-based  $\text{H}^{13}\text{CO}_3^-$  NMR experiment (Figure 5), as reported by Davis and coworkers<sup>10</sup>. In this experiment, NaCl-encapsulated liposomes were suspended in a  $\text{NaH}^{13}\text{CO}_3$  buffer. Then paramagnetic  $\text{Mn}^{2+}$  was added to the extravesicular solution to broaden the  $^{13}\text{C}$ -NMR signal of extravesicular  $\text{H}^{13}\text{CO}_3^-$  to the baseline, which allowed the discrimination of the extravesicular and the intravesicular  $\text{HCO}_3^-$ . After the addition of **CM3**, the  $^{13}\text{C}$ -NMR signal of  $\text{H}^{13}\text{CO}_3^-$  was recovered, indicating an influx of the extravesicular  $\text{H}^{13}\text{CO}_3^-$ . As a negative control, the addition of DMSO did not restore the  $\text{H}^{13}\text{CO}_3^-$  NMR signal, indicating no influx of the extravesicular  $\text{H}^{13}\text{CO}_3^-$ .

Because the amide NH units of  $\alpha$ -aminoxy acid residues are more acidic than regular amide NH groups, they are expected to be better hydrogen bond donors to interact with anions.  $\alpha$ -Aminoxy acid-containing compound **CM1** indeed has higher acidity ( $\text{pK}_a$  8.3, Figure S4) and  $\text{Cl}^-$  binding affinity ( $K > 1 \times 10^5 \text{ M}^{-1}$ ) than  $\alpha$ -amino acid-containing compounds **CM3** and **CM4** (with  $\text{pK}_a > 10$ ). However, the  $\text{Cl}^-$  transport activities of **CM3** and **CM4** were found to be superior to that of **CM1**. This result suggests that the  $\text{Cl}^-$  binding affinity does not correlate with the  $\text{Cl}^-$  transport activity. Instead, the ability of channel assembly from small molecules in non-polar lipid environment may be more important than the ion binding affinity.

To explore the potential biomedical application of **CM3**, we investigated the Ussing-chamber based short-circuit current response of **CM3** in Calu-3 and CFBE41o- epithelial monolayers, which express functional CFTR and F508del-mutated CFTR, respectively<sup>11</sup>. Two batches of Calu-3 monolayers were used, one with low basal current ( $6.4 \pm 0.8 \mu\text{A}/\text{cm}^2$ ,  $n = 30$ ) and the other one with high basal current ( $19.82 \pm 1.28 \mu\text{A}/\text{cm}^2$ ,  $n = 32$ ). In both monolayers, **CM3** elicited short-circuit current increase (Figures 6a and 6b; Figures S6 and S7). Calu-3 monolayers were then pretreated with different channel inhibitors (Figure S6) to explore the ionic nature of short-circuit current increase: CFTR<sub>inh</sub>-172 inhibited apical CFTR conductance; bumetanide blocked  $\text{Cl}^-$  uptake through sodium potassium chloride cotransporter (NKCC); acetazolamide suppressed intracellular carbonate anhydrase (responsible for bicarbonate synthesis in cells). It was found that the short-circuit current increase elicited by **CM3** was CFTR-independent, strongly chloride-dependent and influenced by the presence of extracellular bicarbonate ions or intracellular bicarbonate ion synthesis in both batches of Calu-3 monolayers (Figures 6a and 6b; Figures S6 and S7).

In CFBE41o- cell monolayers with homozygous F508 mutation, **CM3** also induced chloride-dependent short-circuit current increase (Figure 7). After pretreatment with anion exchange inhibitor DIDS or epithelial sodium channel (ENaC) inhibitor amiloride, the short-circuit current response of **CM3** was not greatly affected (Figure S8). However, when the chloride gradient was removed, the short-circuit current increase was almost abolished (Figure S8), indicating the contribution of chloride to the short-circuit current response. Therefore, we concluded that **CM3** restored the dysfunctional chloride secretion caused by F508del mutant CFTR in CFBE41o- cell line.

In summary, **CM3** has been found to self-assemble to form chloride channel in lipid bilayers and mediated  $\text{Cl}^-/\text{HCO}_3^-$  transport across liposome membranes. In Ussing-chamber based short-circuit current measurements, **CM3** has been shown to elicit short-circuit current increase in Calu-3 epithelial monolayers, which could be attributed to the secretion of chloride, and influenced by bicarbonate ions. It can also restore the chloride secretion in CFBE410- monolayers with F508del

mutant CFTR. This discovery opens up opportunity for the treatment of channelopathies caused by dysfunction of chloride and bicarbonate channels, notably cystic fibrosis.

We acknowledge financial supports from The University of Hong Kong and the Hong Kong Research Grants Council Collaborative Research Fund (HKU 2/06C and HKU8CRF10).

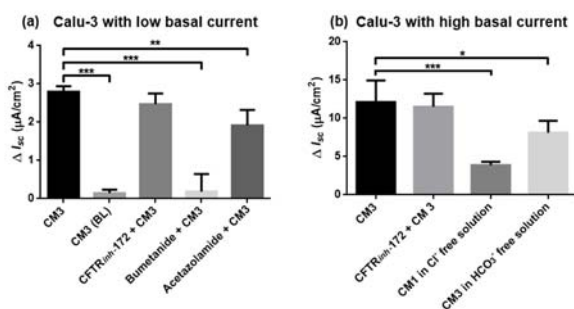


Figure 6. Accumulated data of Ussing-chamber based short-circuit current measurements ( $n = 4$ ). For (a) and (b), short-circuit current was measured in Calu-3 monolayers with low and high basal current, respectively. Unless otherwise indicated, Calu-3 monolayers were bathed bilaterally with the Krebs-Henseleit solution. Each column represents the mean  $\pm$  S.D. ( $n = 4$ ). \*\*\* $p < 0.001$ , \*\* $p < 0.005$ , \* $p < 0.01$ , Quantitative differences between extract groups values were statistically analyzed using one-way ANOVA with a multiple comparison post hoc test by the Bonferroni method.

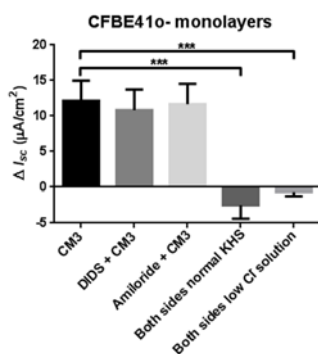


Figure 7. Accumulated data of Ussing-chamber short-circuit current measurement of **CM3** in CFBE410- monolayers ( $n = 4$ ). Without special notification, CFBE410- monolayers were bathed with basolateral to apical chloride gradient. Each column represents the mean  $\pm$  S.D. ( $n = 4$ ). \*\*\* $p < 0.001$ , Quantitative differences between group values were statistically analyzed using one-way ANOVA with a multiple comparison post hoc test by the Bonferroni method.

## Notes and references

- 1 J. R. Casey, *Biochem. Cell Biol.* 2006, **84**, 930.
- 2 D. Sterling and J. R. Casey, *Biochem. Cell Biol.* 2002, **80**, 483; E. Cordat and J. R. Casey, *Biochem. J.* 2009, **417**, 423.
- 3 J. Y. Choi, D. Muallem, K. Kiselyov, M. G. Lee, P. J. Thomas and S. Muallem, *Nature* 2001, **410**, 94.
- 4 N. M. Koropatkin, D. W. Koppelaar, H. B. Pakrasi and T. J. Smith, *J. Biol. Chem.* 2007, **282**, 2606.
- 5 X. Li, B. Shen, X.-Q. Yao and D. Yang, *J. Am. Chem. Soc.* 2007, **129**, 7264; B. Shen, X. Li, F. Wang, X. Yao and D. Yang, *PLoS One* 2012, **7**, e34694; X. Li, B. Shen, X.-Q. Yao and D. Yang, *J. Am. Chem. Soc.* 2009, **131**, 13676.
- 6 H. Zha, B. Shen, K. Yau, S. Li, X. Yao and D. Yang, *Org. Biomol. Chem.* 2014, **12**, 8174.
- 7 N. Busschaert and P. A. Gale, *Angew. Chem.* 2013, **52**, 1374; N. Busschaert, M. Wenzel, M. E. Light, P. Iglesias-Hernández, R. Pérez-Tomás, and P. A. Gale, *J. Am. Chem. Soc.* 2011, **133**, 14136; B. D. de Greñu, P. I. Hernandez, M. Espona, D. Quiñero, M. E. Light, T. Torroba, R. Pérez-Tomás and R. Quesad, *Chem-Eur. J.* 2011, **17**, 14074; P. A. Gale, R. Pérez-Tomás and R. Quesada, *Acc. Chem. Res.* 2013, **46**, 2801; P. I. Hernandez, D. Moreno, A. A. Javier, T. Torroba, R. Perez-Tomas and R. Quesada, *Chem. Commun.* 2012, **48**, 1556; S. J. Moore, C. J. E. Haynes, J. Gonzalez, J. L. Sutton, S. J. Brooks, M. E. Light, J. Herniman, G. J. Langley, V. Soto-Cerrato, R. Perez-Tomas, I. Marques, P. J. Costa, V. Felix, P. A. Gale, *Chem. Sci.* 2013, **4**, 103; S. J. Moore, M. Wenzel, M. E. Light, R. Morley, S. J. Bradberry, P. Gomez-Iglesias, V. Soto-Cerrato, R. Perez-Tomas and P. A. Gale, *Chem. Sci.* 2012, **3**, 2501; S.-K. Ko, S. K. Kim, A. Share, V. M. Lynch, J. Park, W. Namkung, W. V. Rossom, N. Busschaert, P. A. Gale, J. L. Sessler and I. Shin, *Nat. Chem.* 2014, **6**, 885; J. L. Sessler, L. R. Eller, W. S. Cho, S. Nicolaou, A. Aguilar, J. T. Lee, V. M. Lynch and D. J. Magda, *Angew. Chem. Int. Ed.* 2005, **44**, 5989, V. SotoCerrato, P. M. Manresa, E. Hernando, S. C. Fariñas, A. M. Romero, V. F. Dueñas, K. Sahlholm, T. Knöpfel, M. G. Valverde, A. M. Rodilla, E. J. Lewintre, R. Farràs, F. Ciruela, R. P. Tomás and R. Quesada, *J. Am. Chem. Soc.*, 2015, **137**, 15892.
- 8 A. S. Verkman, R. Takla, B. Sefton, C. Basbaum and J. H. Widdicombe, *Biochemistry* 1989, **28**, 4240.
- 9 B. Hille, *Ionic Channels of Excitable Membranes*, Sinauer Associates: Sunderland, MA, 2001; N. E. Sakmann B, *Annu. Rev. Physiol.* 1984, **46**, 455.
- 10 J. T. Davis, P. A. Gale, O. A. Okunola, P. Prados, J. C. Iglesias-Sánchez, T. Torroba and R. Quesada, *Nat. Chem.* 2009, **1**, 138.
- 11 D. C. Devor, A. K. Singh, L. C. Lambert, A. DeLuca, R. A. Frizzell and R. J. Bridges, *J. Gen. Physiol.* 1999, **113**, 743; J. Shan, J. Huang, J. Liao, R. Robert, J. W. Hanrahan, *Acta Physiologica* 2011, **202**, 523; P. L. Zeitlin, L. Lu, J. Rhim, G. Cutting, G. Stetten, K. A. Kieffer, R. Craig, W. B. Guggino, *Am. J. Respir. Cell Mol. Biol.* 1991, **4**, 313.